Food Science and Engineering
http://ojs.wiserpub.com/index.php/FSE/

Research Article

Effect of Temperature on Drying Kinetics and Quality of Partially Deoiled Chia Flour Wheat Pasta

Aranibar C[1], **Aguirre A**[1,2], **Borneo R**[1,2*]

[1]Institute of Food Science and Technology of Córdoba, National University of Cordoba, Córdoba, Argentina
[2]Faculty of Exact, Physical and Natural Sciences, National University of Córdoba, Córdoba, Argentina
E-mail: rafael.borneo@unc.edu.ar

Received: 16 June 2023; **Revised:** 10 October 2023; **Accepted:** 26 October 2023

Abstract: After chia oil extraction, a by-product, partially-deoiled chia flour (PDCF) with a high nutritional value (high content of fiber, protein, and antioxidant properties) remains. The effect of drying temperature on the quality and drying kinetics of wheat pasta enriched with PDCF was evaluated. Wheat pasta was prepared with different proportions of PDCF (0, 5 and 10%, wheat based) and dried at 45, 55 and 65 °C for 24 hours. Experimental data were fitted to different empirical models. Drying kinetics, drying rate (*DR*), effective moisture diffusivity (*Deff*), pasta cooking parameters, microstructure, textural and color were analyzed. The Midilli model had the most suitable performance to describe pasta drying kinetics behaviour. Pasta enriched with PDCF required higher energy input for drying. High drying temperatures had a great impact on enriched pasta quality. Pasta was darker, opaque, irregular, and porous. Cooking time and cooking losses decreased. Hardness was not affected. The strength and microstructure properties of enriched pasta improved at 65 °C, while the non-enriched pasta properties improved at 55 °C.

***Keywords*:** kinetics, chia flour, modeling, pasta quality, drying heat treatment

Abbreviations

PDCF	partially-deoiled chia flour
MC	moisture content
MR	moisture ratio
t	dying time
M_t	moisture content at any point of drying process
M_e	equilibrium moisture content
M_0	initial moisture
$RMSE$	root mean square error
$MR_{pre,i}$	predicted moisture ratio
$MR_{exp,i}$	experimental moisture ratio
N	number of observations
DR	drying rate

DOI: https://doi.org/10.37256/fse.5120243238

Deff	pasta moisture diffusivity
L	critical drying distance
k	drying kinetic constant
A_e	activation energy
OCT	optimum cooking time
WA	water absorption
WG	weight gain
CL	cooking loss
CLSM	confocal laser scanning microscope
GLCM	Gray-Level Co-occurrence Matrix

1. Introduction

Chia seed (*Salvia hispanica* L.) originated in Central and South America. Its present interest to researchers is mainly due to their nutritional composition and their benefits to the human-health. After chia oil extraction, a by-product, partially-deoiled chia flour (PDCF) with a high nutritional value (high content of fiber, protein, and antioxidant properties) remains [1]. Recent years there has been a special growing appeal in the use of this residue to fortified different food products as maize tortillas [2], cookies [3], gluten-free premixes [4] and highly nutritional breads [5].

Pasta is consumed all over the world and is preferred in all age groups. It is a good source of energy, high in complex carbohydrates but low in protein, minerals, vitamins, bioactive compounds and dietary fiber [6]. Pasta can be used as a functional food through the incorporation of healthy components in its formulation. Several studies have shown the viability of fortifying pasta with berries [7], and spirulina [6] beside others. We used PDCF as a source of antioxidants to enhance the nutritional value in pasta and muffins [8-9]. Other researchers [10-11] have used crushed chia seeds for the production of pasta products.

The application of heat air treatments is one of the most important processes in pasta manufacture since it provides the final characteristics of texture and stability during storage. During drying, a phenomenon of mass and energy transport in an unsteady state occurs [12], the initial moisture content (*MC*) of fresh pasta (31% w.b.) reduces to an appropriate final moisture for preservation (11% w.b.), in order to restructure the protein network that embeds around the starch granules. Pasta drying conditions (temperature, drying time and moisture content) could affect its final quality [13]. In this regards, the study of its optimal drying conditions allows in to manufacture good quality pasta, optimizing drying times, the use of energy and reducing costs. Although these investigations have reported the effect of drying temperature on pasta making process, to the best of our knowledge the effect of drying temperature on PDCF-enriched pasta quality has not been studied so far.

In previous studies we have found that the incorporation of PDCF in the pasta manufacture process impacts on technological quality [8-9]. In general, the amount of material to be added to a food formulation is a compromise between the intended improvement of nutritional quality and the sensory and functional properties of the final product. In this context, the aim of this work was to study the drying kinetics of pasta and the effect of drying temperature on pasta structural characteristics.

2. Materials and methods

2.1 *Obtaining PDCF and manufacturing of pasta*

Commercial wheat flour (*Triticum aestivum*) was purchased from Molino San José, José Minetti & CIA Ltda. (Córdoba-Argentina). Chia seeds (*Salvia hispanica* L.) were purchased in a local market. PDCF was obtained by a screw pressing [14]. A small-scale standardized laboratory procedure was used for pasta manufacture [1]. Pasta was prepared with different concentrations of PDCF (0, 5 and 10% PDCF, respectively, weight flour basis). The 0.0% PDCF sample corresponds to a 100% wheat flour pasta. For each formulation pasta flour, water, and salt (50 g, 22.5 g, and 1.0 g, respectively) were mixed in a Hobart bench top mixer (Hobart Inc., Troy, OH, USA) until the dough had an adequate consistency for lamination. Dough was divided by hand in appropriate size and was laminated using a pasta home scale size lamination machine (Drago, Inc., China) using a 3-step procedure: hand lamination, up to approximately 10-mm thickness; roll lamination, up to a 5-mm thickness; and final roll lamination to a 2-mm thickness (final pasta thickness). Laminated pasta sheets were cut using a cutting roll (2-mm wide) obtaining the pasta.

2.2 *Drying kinetics study*

Pasta samples (10 g) were dried on homemade aluminum perforated trays in two steps. The first stage, termed pre-drying, (30 min, 30 °C, forced air ventilation) in a laboratory drier (Memmert Model 600 D060602, Germany). Then, a second stage (termed drying) was used (FAC model CDH4060, Argentina) with moisture control (75%) and at 45, 55 and 65 °C for 24 hours. The weight of samples (quadruplicates) was taken during the pre-drying stage at intervals of 10 min. During the drying stage (second drying step) samples were taken each 15 minutes during the first hour and every 60 min until the 24 hours maximum of drying was reached. Moisture content (*MC*) was determined according to the official method 44-19 of the American Association of Cereal Chemists (AACC) [15]. The results were expressed in g of water lost/100 g of sample. Dried pasta was stored in airtight bags at room temperature until needed.

2.3 *Mathematical modeling*

Moisture ratio (*MR*) as a function of drying time (*t*) was computed and plotted using *MC* values for each temperature and determined according equation 1.

$$MR = \left(M_t - M_e\right)/M_0 - M_e \quad (1)$$

Where M_t, M_e and M_0 are the moisture content (*MC*, kg water/kg dry mater) at any point of drying process, equilibrium and initial time, respectively. A linear and non-linear regression method was used. The experimental data (*MR* vs drying time) were fitted to seven mathematical models for thin layer drying curves (Table 1) .

Table 1. Parameters and statistical analysis of control pasta experimental models

0% PDCF								
Model		T °C	Constants and coefficients				R^2	RMSE
			a	k	c	n		
Henderson and Pabis	*MR* = a*EXP(-k*t)		1.0692	0.0054			0.9865	0.0374
Logarithmic	*MR* = a*EXP(-kt) + c		1.0765	0.0053	-0.0099		0.9869	0.0382
Midilli	***MR* = a*EXP(-k*t^n) + bt**		1.0191	0.0011	6.0437E-06	1.2978	0.9957	**0.0228**
Wang and Singh	*MR* = 1 + b*t + a*t^2	45	1.4053E-06	-0.0027			0.8673	0.1174
Lewis	*MR* = EXP(-k*t)			0.0051			0.9821	0.0417
Modified page	*MR* = EXP(-(k*t)^n)			0.005		1.3172	0.9952	0.0224
Page	*MR* = EXP(-k*t^n)			0.0009		1.3172	0.9952	0.0224

Table 1. (cont.)

0% PDCF								
Model		T °C	Constants and coefficients				R^2	RMSE
			a	k	c	n		
Henderson and Pabis	*MR* = a*EXP(-k*t)		1.0275	0.0104			0.9869	0.033
Logarithmic	*MR* = a*EXP(-kt) + b		1.0248	0.0105	0.0036		0.9869	0.033
Midilli	***MR* = a*EXP(-k*t^n) + bt**		**1.007**	**0.0026**	**6.3331E-06**	**1.2816**	**0.9923**	**0.0262**
Wang and Singh	*MR* = 1 + b*t + a*t^2	55	1.7156E-06	-0.0032			0.258	0.2401
Lewis	*MR* = EXP(-k*t)			0.0102			0.9861	0.0318
Modified page	*MR* = EXP(-(k*t)^n)			0.0096		1.2806	0.992	0.025
Page	*MR* = EXP(-k*t^n)			0.0026		1.2806	0.992	0.025
Henderson and Pabis	*MR* = a*EXP(-k*t)		1.0310	0.0117			0.9837	0.0352
Logarithmic	*MR* = a*EXP(-kt) + b		1.0264	0.0118	0.0043		0.9839	0.0362
Midilli	***MR* = a*EXP(-k*t^n) + bt**		**1.0022**	**0.0015**	**9.1736E-06**	**1.4323**	**0.9952**	**0.0205**
Wang and Singh	*MR* = 1 + b*t + a*t^2	65	1.7476E-06	-0.0032			0.1015	0.2614
Lewis	*MR* = EXP(-k*t)			0.0114			0.9829	0.0349
Modified page	*MR* = EXP(-(k*t)^n)			0.0104		1.4243	0.9945	0.0205
Page	*MR* = EXP(-k*t^n)			0.0015		1.4243	0.9945	0.0205

* *MR*: moisture ratio; k: drying constant; n, a, b and c are equations constants

To identify the best fit model, the highest coefficient of determination (R^2) and the lowest root mean square error (*RMSE*) were considered. Equation 2 shows the *RMSE* calculation.

$$RMSE = \left(\sum_{i=1}^{N} \begin{pmatrix} MR_{pre,i} \\ -MR_{\exp,i} \end{pmatrix}^2 / N \right)^{0.5} \tag{2}$$

Where $MR_{pre,i}$ and $MR_{exp,i}$ are the *i-th* predicted and experimental moisture ratio, respectively. *N* is the number of observations.

2.4 *Drying rate*

Equation 3 was used to determine the drying rate (*DR*).

$$DR = -(dMbs/dt) = -((M_{t+\Delta t}) - Mt)/(t_{i+1} - t_i) \quad (3)$$

Where, $M_{t+\Delta t}$ is the moisture content on dry basis (kg water/kg db) at time (t_i) + time difference (min); *DR* is drying rate (kg water/kg min) and *t* is drying time (min).

2.5 *Effective moisture diffusivity*

The pasta moisture diffusivity (*Deff*) was calculated by solving the diffusion equation of Fick's law for a thin layer. Thus, it was considered that the moisture loss is uniformly distributed on both sides of pasta, the Crank equation (Equation 4) was applied [16-17].

$$MR = \left(8/\pi^2\right)\sum_{n=0}^{\infty}\left(1/(2n+1)^2\right)\exp\left(\left(-\left((2n+1)^2\,\pi^2/4L^2\right)\right)*(Deff*t)\right) \quad (4)$$

Where, *MR* is the moisture ratio (kg water/kg db); *Deff* is the effective moisture diffusivity (m^2/s); *t* is drying time (min); *L* is the critical drying distance in (m) (1/2 of pasta thickness). Considering pasta as a thin layer and a drying over long periods of time, equation 4 can be simplified as equation 5.

$$MR = \left(8/\pi^2\right)\exp-\left(\left(\pi^2\,Deff*t\right)/\left(4*L^2\right)\right) \quad (5)$$

2.6 *Activation energy*

The relationship of temperature vs the diffusion coefficient (*Deff*) and the drying kinetic constant (*k*) was determined following the Arrhenius model (Equation 6) .

$$k = k_0 * \exp^{(-(Ae/R*T))} \quad (6)$$

The Arrhenius equation was linearized and *Ln (Deff)* and *Ln* (*k*) were graphed as a function of 1/*T*, the slope obtained in the line equation was used to calculate activation energy (A_e).

$$LnDeff = LnD_0 - (A_e/R)*(1/T) \quad (7)$$

Where, *k* is drying kinetic constant (min-1); k_0 and D_0 are pre-exponential constants (min^{-1} and m^2/s respectively); A_e is activation energy (kJ/mol); *T* is absolute drying temperature (°K); *R* is the universal gas constant (8.314×10^{-3} kJ/mol K).

2.7 *Pasta cooking parameters*

Cooking quality parameters of pasta were evaluated according to method 16-50 of the AACC [15]. Optimum cooking time (OCT), water absorption (WA), weight gain (WG), and cooking loss (CL) were assessed.

2.8 *Texture and color analysis*

Texture analysis of cooked pasta was performed using an INSTRON Texturometer (Model 3,342, Norwood, MA, USA) equipped with a 500 N cell. Breaking force (BF) of each strand of uncooked pasta was evaluated by the three-point bending test [15]. Firmness and gumminess of cooked optimum time pasta were calculated using Application Study Ref N002/P35 (Stable Micro System, Surrey, UK). A cylindrical probe (AP/35) was used to compressed twice 4 strands of cooked pasta (5 cm long each) at fixed 60% strain; the results were expressed in Newtons. Pasta color was determined using a Minolta 508d spectrophotometer (Ramsey, NJ, USA) according to method 14-22 [15], which details each color in the CIE Lab coordinates color space: L* (lightness), a* (red-green) and b* (yellow-blue).

2.9 *Textural analysis of pasta images obtained by microscopy*

The microstructural characteristics of the inner structure of raw pasta were evaluated using an Olympus LEXT OLS4000 3D confocal laser scanning microscope (CLSM). The Image J program (National Institutes of Health, USA) using a second order statistical algorithm called Gray-Level Co-occurrence Matrix (GLCM) was used for textural analysis of the images. The images obtained in JPEG were corrected to 8 Bit and later binarized in two colors, black and white, allowing quantified the microstructural differences between the samples. The following dimensionless parameters were obtained from the analysis of the images: Energy also called Uniformity or Angular second moment which measures the textural uniformity, entropy which measures the disorder or complexity of an image, homogeneity also called as Inverse Difference Moment and fractal dimension using the Fractal Box count algorithm in the Image J software, which provided a numerical parameter that described the morphology and texture of the images with irregular and complex structures.

2.10 *Statistical analysis*

A linear and non-linear regression method was used to fit pasta drying kinetics data. The adjusted coefficient of determination (R^2), was used to evaluate the quality of the fit. The results were analyzed using the InfoStat Statistical Software (Facultad de Ciencias Agropecuarias, UNC, Argentina), significant differences between samples were evaluated with Analysis of Variance (ANOVA) ($p < 0.05$). The results were compared using the DGC method [18]. The statistical analysis was executed using SigmaPlot software (v.12.5, SigmaPlot Software, Chicago, IL, USA). Each analysis was accomplished in three replicates.

3. Results and discussion

3.1 *Pasta drying conditions*

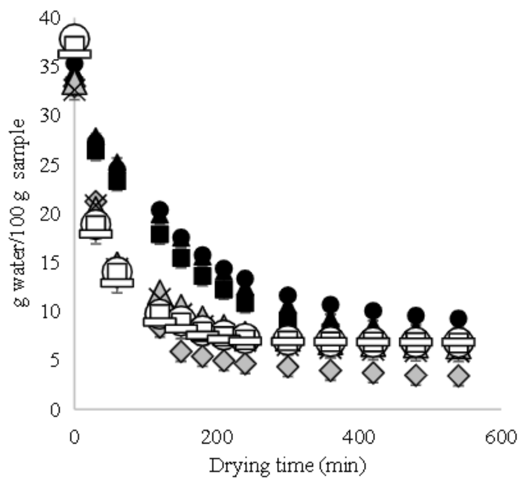

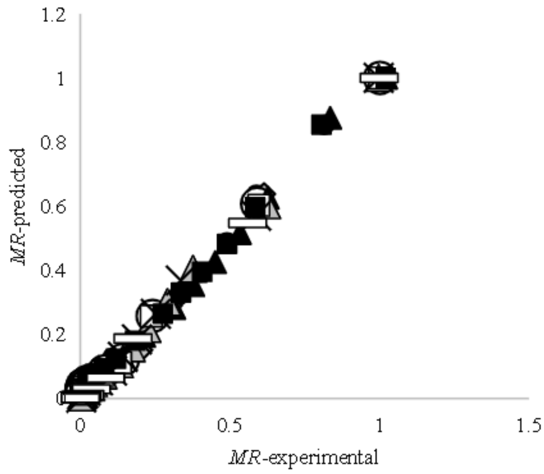

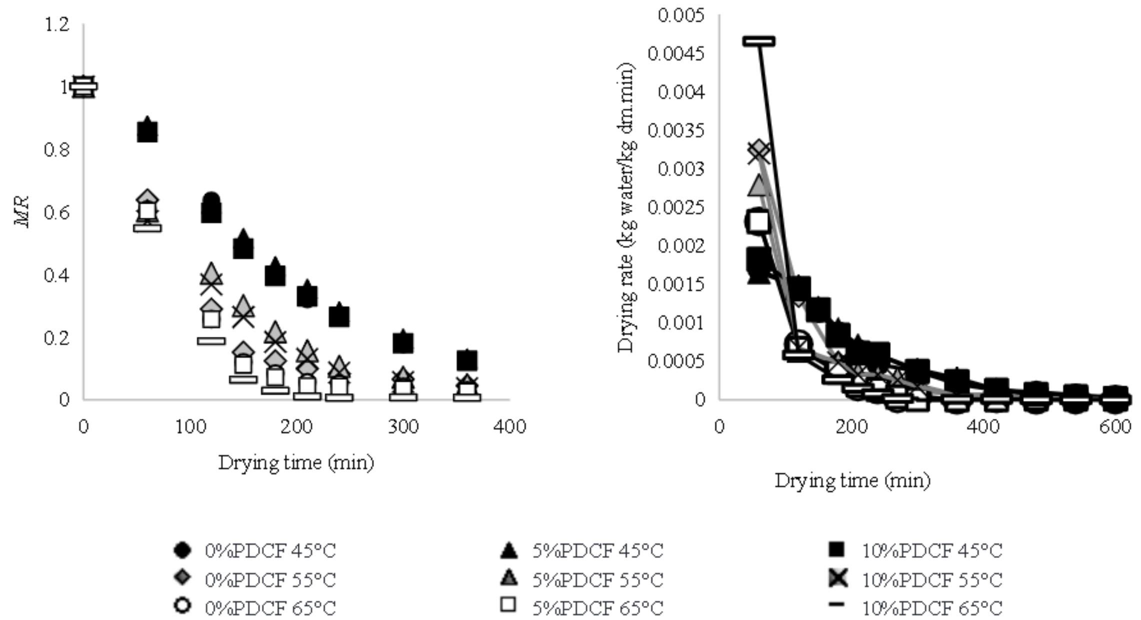

Figure 1. (a) Moisture ratio (*MR*) variation as a function of drying time at different temperatures (b) Relationship between *MR* and drying time at different temperatures (c) Experimental vs predicted *MR* by the Midilli et al. (2002) model at different temperatures (d) Pasta drying rate and drying time relationship at different temperatures.

Figure 1a shows that the highest moisture loss occurred during the first six hours of drying process (360 min). As there is more water available in the pasta at the beginning of the process, the water is more available to be evaporated. Contrary to this, at the end of the process the decrease in moisture content was increasingly slower until reaching equilibrium moisture content after 24 h of the process. Moreover, the *MC* reduction during the drying time of each sample (0, 5 and 10% PDCF) was influenced by different drying temperatures (45, 55 and 65 °C) (Figure 1b). The higher the drying air temperature was, a greater loss of moisture occurred as a result of the greater heat transfer from the pasta surface to the inner. High temperatures decreased the drying time, since after the first 5 h of drying at 45 °C, after the first 2 hours of drying at 55 °C and after the first hour and a half of drying at 65 °C, the pasta reached acceptable storage moisture values (<12.5%), at which point the moisture content began to decrease at a lower rate.

3.2 *Pasta drying mathematical models*

The adjusted determination coefficient values (R^2) of the models evaluated had a great variability (ranging from 0.258 to 0.999). Root mean square error (*RMSE*) values were in the range of 0.007 to 0.264 (Table 1 as representative of control sample-other data not shown). The Midilli and Page models showed the best performance, and also high capacity to describe pasta behavior, showing the highest values of the R^2 and the lowest values of *RMSE*. However, we did not choose the Page model because the R^2 values were lower than in Midilli. The Page model has been already considered by other authors as the one with the best fit for a thin layer drying process of pepper slices [17] and yacón [19] among others. However, López-Mejía et al. [20] showed that the Henderson and Pabis and the Logarithmic models described in a better way the pumpkin enriched pasta drying kinetics and the Page model was chosen to represent spinach pasta drying kinetics [21].

The parameters and statistics related to the best fit model (Midilli) were grouped and are detailed in Table 2. The drying air temperature and rate are the variables that significantly affect the "k" parameter in a thin layer drying equation, and is usually related with *Deff* coefficient. On the other hand, the "n" parameter behaves according to: the relative moisture of the air, the product initial moisture content, the nature of the product and the drying conditions, which shows the internal resistance of the product to the drying process.

Table 2. Constants calculated by Midilli model

Midilli	Constants and coeficients					R^2	RMSE
MR = a*EXP(-k*t^n) + bt	T°C	a	k	c	n		
0% PDCF	45	1.0191	0.0011	6.0437E-06	1.2978	0.9957	0.0228
	55	1.007	0.0026	6.3331E-06	1.2816	0.9923	0.0262
	65	1.0022	0.0015	9.1736E-06	1.4323	0.9952	0.0205
5% PDCF	45	1.023	0.0011	9.2907E-06	1.2743	0.9951	0.0243
	55	0.9973	0.0062	1.1776E-06	1.0562	0.9979	0.0137
	65	1.0007	0.0012	6.6238E-06	1.4816	0.9964	0.018
10% PDCF	45	1.0212	0.0015	0.000010402	1.2367	0.9951	0.0237
	55	0.9974	0.0074	1.1201E-06	1.0424	0.9981	0.0129
	65	0.9991	0.0009	6.9312E-07	1.58	0.9994	0.0075

R2: coefficient of determination, k: drying constant; n, a, b and c are equations constants; t: drying time; RMSE: lowest root mean square error

Based on the chosen model, the experimental data (MR_{exp}) were compared with the predicted data (MR_{pre}) by the Midilli model. Figure 1c shows the data of samples grouped in a straight line justifying the choice of the model.

3.3 *Drying rate (DR)*

As shown in Figure 1c, *DR* reported two types of behaviors: 1) a sharp increase in *DR* at the beginning of the process (first two hours of drying) and 2) a subsequent gradual decrease in *MC*. This variation is due to the fact that the *MC* was initially high (35% ± 3), in this first stage the pasta surface is saturated with water so there is greater evaporation accelerating the dehydration rate. On the other hand, at the end of this period, the water transfer from pasta inner was increasingly slower than the water vaporization to the air, which is why the drying rate decreased until reaching moisture equilibrium. *DR* was governed by temperature so higher values were obtained at higher temperatures. Previous researchers have also established a similar behavior in all conditions of temperature (30 to 90 °C) and relative humidity (50% to 80%) [22]. Pasta transformation occurs from a gummy state to a glassy state with a decrease in *MC* during drying [23]. There are similarities with the results described by starch [24], and strawberries [25].

Table 3. Effective moisture diffusivity (Deff) of samples at different temperatures (up-left). Color and breaking force of dried pasta (up-right). Cooking characteristics of pasta samples (down)

Uncooked pasta							
PDCF (%)	T°	Deff (m^2/s)	R^2	L*	a*	b*	BF (N)
0	45°C	6.36E-09	0.98	78.1 ± 1.02 a	1.20 ± 0.16 a	15.84 ± 0.2 a	2.67 ± 0.21 a
	55°C	1.18E-08	0.97	77.6 ± 0.12 a	1.28 ± 0.08 a	15.61 ± 0.39 a	3.85 ± 0.33 b
	65°C	1.44E-08	0.94	70.4 ± 0.73 b	1.95 ± 0.12 b	14.34 ± 0.25 b	1.48 ± 0.33 c
5	45°C	6.26E-09	0.98	74.0 ± 1.6 a	1.39 ± 0.16 a	13.10 ± 0.04 a	2.20 ± 0.65 a
	55°C	1.00E-08	0.99	74.6 ± 0.85 a	2.06 ± 0.03 b	13.28 ± 0.26 a	2.46 ± 0.38 a
	65°C	1.55E-08	0.93	65.8 ± 1.91 b	2.09 ± 0.01 b	13.35 ± 0.25 a	2.91 ± 0.45 a
10	45°C	6.00E-09	0.98	72.2 ± 1.37 a	2.07 ± 0.04 a	11.90 ± 0.2 a	1.96 ± 0.27 a
	55°C	1.04E-08	0.99	73.2 ± 0.89 a	2.32 ± 0.04 a	11.38 ± 0.39 a	1.90 ± 0.61 a
	65°C	2.36E-08	0.93	64.10 ± 3.09 b	2.62 ± 0.29 b	11.56 ± 0.25 a	2.41 ± 0.99 b

Cooked pasta							
PDCF (%)	T°	OCT	WG (%)	CL (%)	WA (g/100)	Firmness (N)	Gumminess (N)
0.00	45°C	12.75 ± 0.21 a	2.57 ± 0.02 a	7.3 ± 0.65 a	157.2 ± 2.47 a	7.08 ± 0.77 a	4.75 ± 0.26 a
	55°C	10.40 ± 0.14 b	2.83 ± 0.10 b	7.23 ± 0.12 a	183.00 ± 10.24 b	6.34 ± 0.59 a	3.94 ± 0.66 b
	65°C	11.27 ± 0.05 c	2.22 ± 0.02 c	5.11 ± 0.25 b	121.7 ± 2.12 c	6.35 ± 0.53 a	4.96 ± 0.33 a
5.00	45°C	11.33 ± 0.18 a	2.85 ± 0.19 a	7.38 ± 0.29 a	185.00 ± 19.43 a	6.86 ± 0.75 a	6.09 ± 0.67 a
	55°C	10.14 ± 0.06 b	2.69 ± 0.04 a	6.82 ± 0.3 a	169.00 ± 4.36 a	6.92 ± 0.75 a	5.01 ± 0.59 b
	65°C	9.42 ± 0.04 c	2.16 ± 0.02 b	5.89 ± 0.13 b	115.7 ± 1.67 b	7.19 ± 0.52 a	5.01 ± 0.48 b
10.00	45°C	11.04 ± 0.06 a	2.52 ± 0.04 a	7.42 ± 0.17 a	15.002 ± 3.89 a	6.88 ± 0.68 a	6.59 ± 0.66 a
	55°C	10.03 ± 0.04 b	2.79 ± 0.01 b	7.78 ± 0.12 a	178.8 ± 0.77 b	7.16 ± 0.67 a	5.76 ± 0.75 a
	65°C	9.76 ± 0.28 b	2.31 ± 0.03 c	5.49 ± 0.06 b	131.3 ± 3.13 c	7.16 ± 0.38 a	6.42 ± 1.02 a

Values with the same letter are not significantly different ($p < 0.05$) according to the DGC test; PDCF = partially deoiled chia flour. color parameters (L*, b* and a*), BF: breaking force, T°: temperature. Optimum cooking time (OCT), (WA) water absorption, (WG) weight gain, (CL) cooking loss.

3.4 *Effective moisture diffusivity (Deff)*

The *Deff* for each sample against the different temperatures evaluated (45, 55 and 65 °C) are shown in the Table 3. The values ranged from 5.99 × 10^{-09} to 2.36 × 10^{-08} and presented high R^2 values. These results were in concordance within the *Deff* range (10^{-10} to 10^{-7}) found from other authors [8,21] for pasta samples. This variation of *Deff* ranges found in pasta products is given by the effect of experimental procedures conditions, model proposed, sample thickness, composition and structure [26]. A clear dependence of *Deff* and drying temperature was found. *Deff* values increased significantly when the drying temperature was higher. The increase in temperature contributed to a greater water diffusion favoring the drying process. The aforementioned studies also reported an increase in *Deff* as a function of drying temperature. If we analyze the samples for the addition of PDCF, the *Deff* values at 45 °C decreased as the PDCF was higher due to its water retention capacity. However, the PDCF behavior was antagonistic to that observed at 45°C when increasing the drying temperature (55 and 65 °C), causing a decrease in PDCF water retention capacity allowing the release of retained water and increasing the diffusion of moisture inside pasta.

3.5 *Activation energy*

The activation energy for non-enriched pasta (0% PDCF) was 36.64 kJ/mol, for 5% PDCF pasta was 42.45 kJ/mol and for 10% PDCF pasta was 59.06 kJ/mol. All samples obtained good fits (R^2: 0.92, 0.99, 0.99, respectively) (Figure 2). From this point, PDCF pasta needed more energy to remove moisture from its inner for a typical drying process (45, 55 and 65 °C). Other authors reported A_e values in a range from 19.34 to 37.71 kJ/mol for spinach pasta [21] and rice noodles. In fact, the values may vary due to the conditions of processing, storage and the source of raw materials [27].

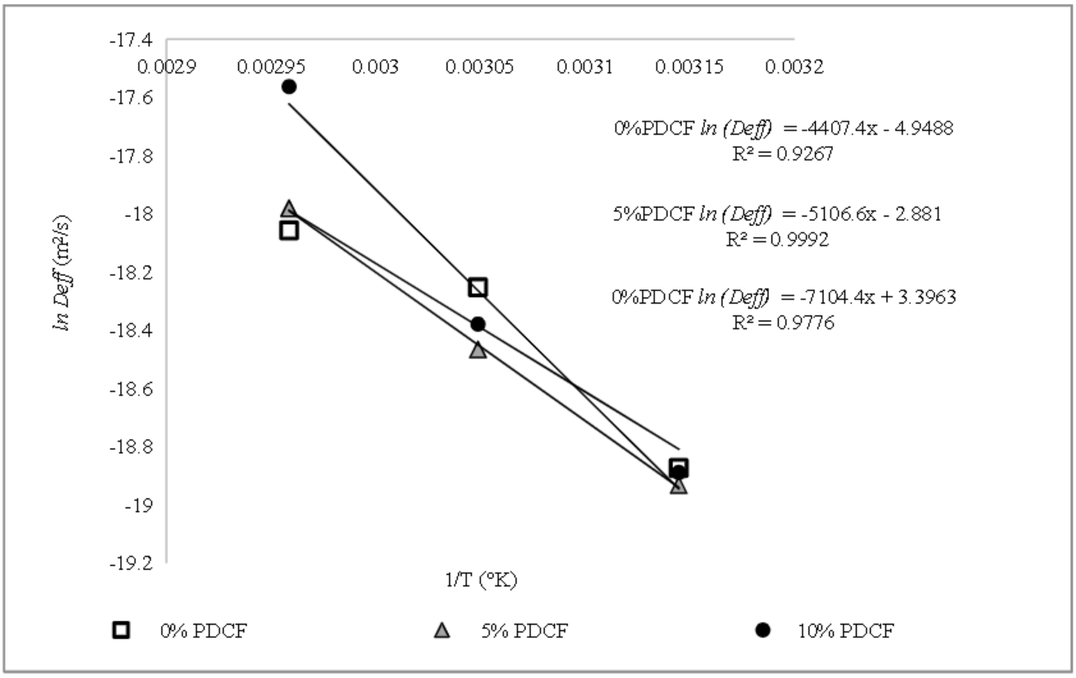

Figure 2. Linear regression analysis for *ln Deff* as a function of 1/T by curve fitting. The slope obtained in the equation of the line gives the value of activation energy

3.6 *Pasta cooking parameters*

3.6.1 *Effects on texture and color of raw pasta*

To evaluate the impact of pasta drying temperatures, the main quality parameters analyses of uncooked pasta (color and breaking force) were carried out (Table 3). Regarding color values and analyzing each sample as a separate entity, the results indicate that as the drying temperature increases, the L* parameter (brightness) significantly ($p < 0.05$) decreases from 78.09 to 70.36 for control sample, from 73.97 to 65.77 for 5% PDCF and from72.20 to 64.10 for 10% PDCF. This implies that drying at 65 °C leads to pasta surface looks opaque. The redness parameter a* ranged from 1.20 and 2.62, and opposite to L*, the highest values were obtained by the samples dried at 65 °C. The increase in redness could be linked to non-enzymatic browning reactions as a result of drying at high temperatures [28]. Control sample dried at 65 °C pointed out negative yellowness (b*) values. In case of fortified samples, as the original color of PDCF is brown, the difference in yellowness was not significantly detected ($p < 0.05$).

BF is an indication of how strong the pasta is during handling and storage. The results ranged from 1.48 to 3.85 (Table 3), control sample dried at 55 °C presented the highest values being the most resistant sample compared to the rest. Gull et al. [8] also observed that spaghettis dried at 50 °C with 70% RH showed the best BF values. In case of enriched pasta (5% PDCF), no significant differences were found between them, but a significant increase was observed for 10% PDCF sample dried at 65 °C. Another study [22] pointed out that although they have not found significant differences in the resistance to brake to their pasta samples dried at 50, 70 and 85 °C, the sample dried at very high temperature showed more resistance. They argued that drying at high temperatures favors the formation of disulfide bonds, increasing the strength of protein network and pasta structure.

3.6.2 *Effects on quality properties of cooked pasta*

Table 3 also shows the quality properties of cooked pasta dried at different temperatures. Although the BF of control pasta dried at 55 °C was the highest (Table 3), the drying temperature didn't affect significantly ($p < 0.05$) the final hardness of cooked pasta in any sample. The firmness values obtained varied between 6.34 and 7.19 N.

Optimum cooking time (OCT) varied from 9.42 to 12.75 min, this parameter decreased as the drying temperature increased. Cooking loss (CL), weight gain (WG) and water absorption (WA) decreased as a result of increasing drying temperature, due to a higher porosity of pasta dried at higher temperatures (Figure 3). This tendency found is in concordance to those reported in Chinese noodles [29].

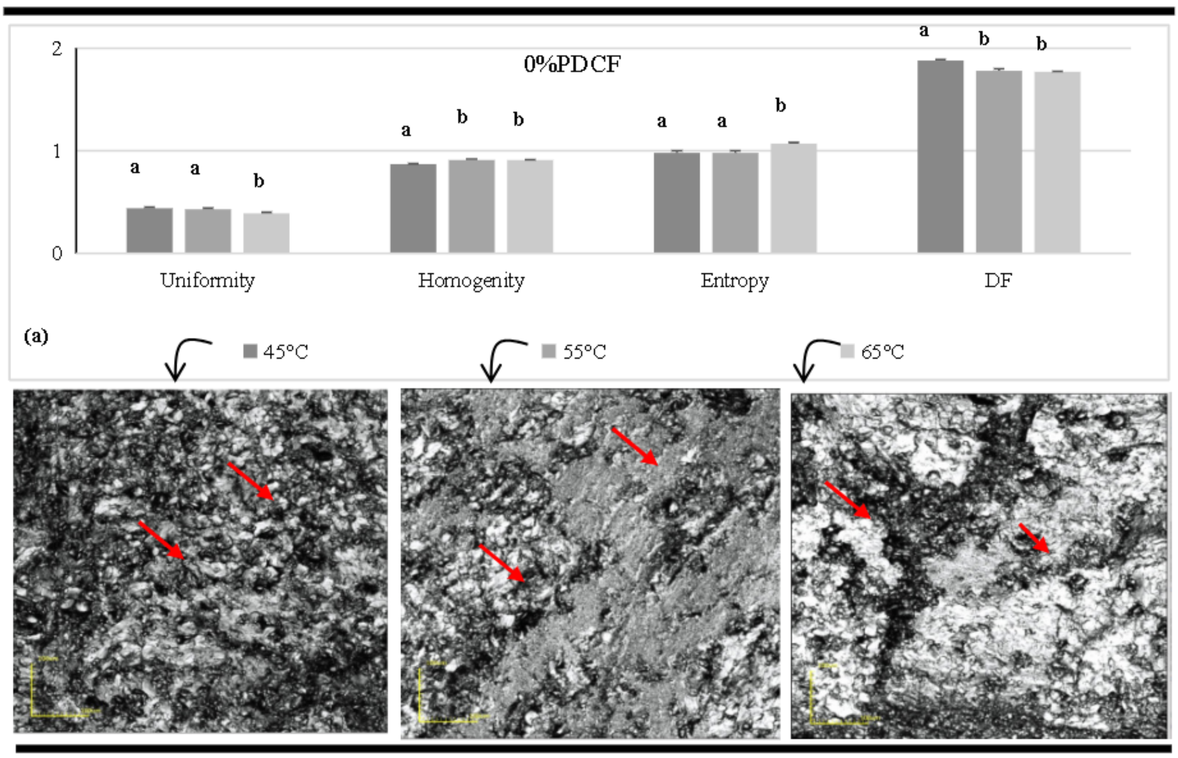

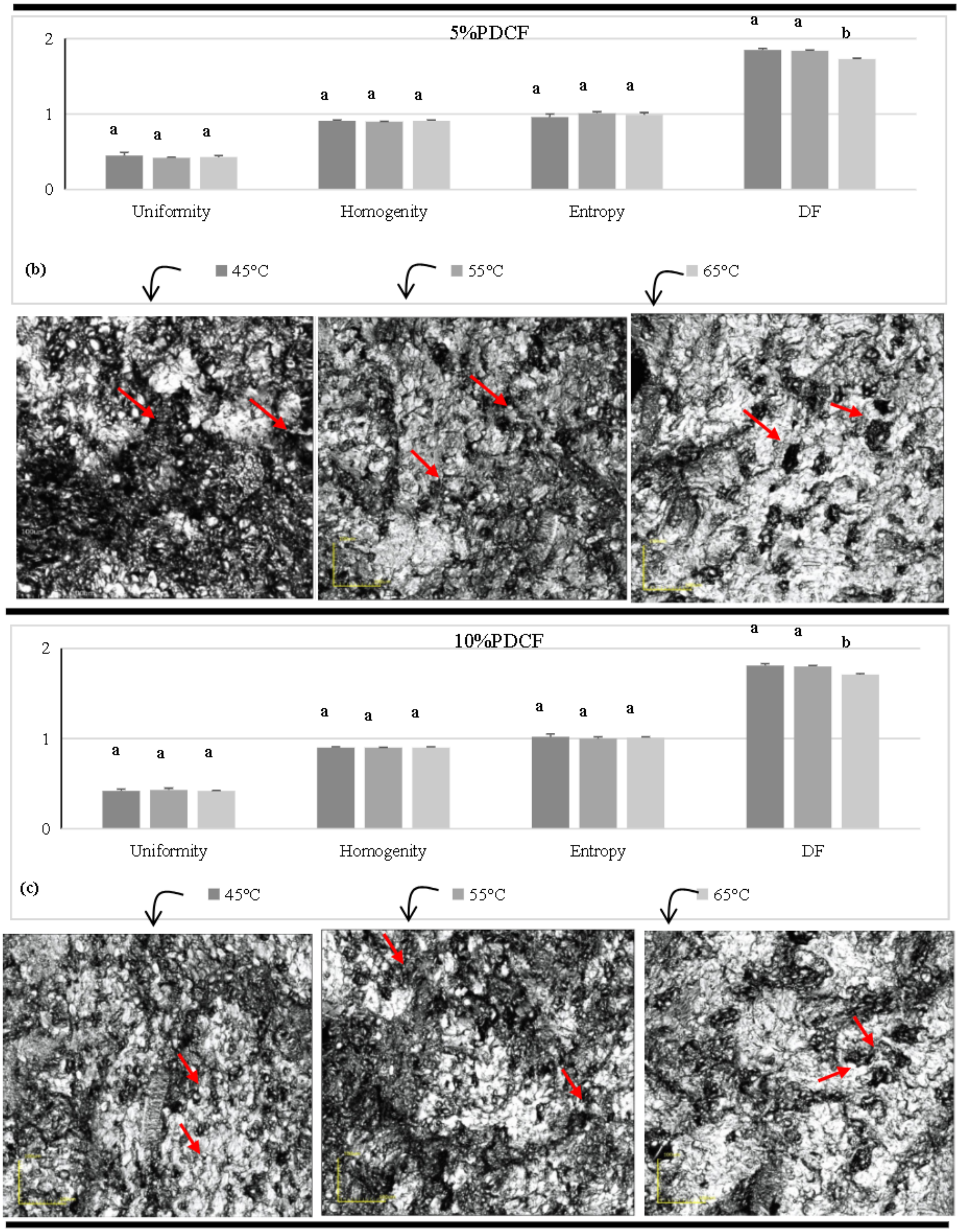

Figure 3. GLCM of confocal images of inner pasta dried at 45, 55 and 65 °C, magnification of 428x. The arrows indicate water evaporation pores. (a) 0%PDCF pasta (b) 5%PDCF pasta (c) 10%PDCF pasta

3.6.3 *Analysis of pasta microstructure dried at different temperatures*

The microphotography of the internal microstructures of dried pasta (Figure 3) revealed an open and porous structure with the presence of empty spaces, indicating evaporation, water transport and its replacement by air during drying. In general, it seems that the pore size of pasta seems to increase as the pasta is dried at higher temperatures (Figure 3, left to right). Drying at low temperatures (45 °C) lead to a slow evaporation and therefore the transport of water is less from pasta inner to the outside, resulting in a structure with smaller pores. This may have occurred because the high temperatures could cause an increase in water vapor pressure giving as a result in a higher mass transfer and thus pore growth during drying. However, the internal structure of control sample dried at 55 °C (Figure 3a), doesn't appear to be porous but rather a more consolidated, compact and dense protein matrix with irregular and almost imperceptible pores. In contrast of this, microphotographs of pasta dried at 65 °C appear to be a porous and brighter structure, demonstrating the presence of a denser and firmer protein network. Other researchers [30] have also found that drying at high temperatures caused the formation of larger and more heterogeneous pores and that the level of gelatinization during the dehydration process produced a great deformation and swelling of the dispersed phase (starch granules). The level of gelatinization during this process is regulated by the denaturation of gluten proteins. These results, combined with the results of BF, firmness and OCT (Table 3), confirmed that the number and size of the pores was crucial to determine the characteristics and quality of pasta.

3.6.4 *Textural analysis of confocal images using GLCM*

The effect of dried temperature on pasta structure is not quite clear from the data shown in Figure 3. However, although some parameters are not statistically significant, some changes can be inferred. The incorporation of PDCF made the pasta internal structure more tortuous and irregular compared to control pasta (confocal images Figure 3). No significant differences were observed in terms of uniformity, homogeneity and entropy values between the enriched pasta dried at different temperatures, but significant differences were found in control pasta. During drying control pasta at 55 °C, its internal structure was affected becoming more compact and complex (Entropy: 0.90 to 1.07), uniformity and homogeneity decreased significantly ($p < 0.05$) from 0.44 to 0.39 and from 0.91 to 0.87, respectively. High values of entropy and low values of uniformity are related to a high state of disorder and a rough surface of the samples. Contrary to this, samples with low values of entropy and high values of uniformity are characterized by smooth textural surfaces. The images obtained by confocal microscopy (Figure 3) in the case of control pasta dried at 55 °C corroborate these results since its internal structure doesn't appear to be so porous but rather compact with irregular and almost imperceptible pores. However, drying at 65 °C significantly decreased the DF values of all samples, resulting in less tortuous internal structures. Other authors have demonstrated that drying at high temperatures (60-100 °C) makes the protein network more continuous and dense [31].

4. Conclusions

The Midilli model presented a satisfactory fit to the experimental data to describe the pasta drying process. The *DR* and the *Deff* coefficients in samples with PDCF were governed by temperatures (55 and 65 °C). As the temperature increases, there is a greater transfer of heat from the pasta surface to its inner, accelerating the internal evaporation of the sample. However, control pasta obtained better drying rate values at 55 °C. Fortified pasta required higher A_e (45 and 59.06 kJ/mol) for a typical drying process be occur compared to non-fortified pasta (36.64 kJ/mol). Drying temperature significantly affected OCT, CL, WG and WA, as a result, pasta dried at higher temperatures appeared to have greater internal porosity (larger pores) while the pores observed in samples dried at lower temperatures appeared to be smaller. The incorporation of PDCF weakened the pasta internal structure when dried at low temperatures. However, its strength and microstructure properties improved when was dried at 65 °C and non-enriched pasta presented better resistance properties, a more compact and dense structure when were dried at 55 °C. Nevertheless, these differences were simplified after cooking. In this sense, the drying temperature affects the strength of dry pasta and not so much the final strength of pasta after cooking.

Author contribution

C.A. was responsible for conducting the experiments, analyzing the data, writing the original draft, visualization, and editing the manuscript. A.A. contributed to the conceptualization, reviewing the manuscript, and funding acquisition. R.B. was in charge of conceptualization, experimental design, funding acquisition, supervision, and manuscript revision.

Aknowledgements

We would like to thank Fernanda Quiroga for her technical help.

Funding sources

This work was supported by CONSOLIDAR Project SECyT, Universidad Nacional de Córdoba-Argentina [33620180100099CB], and Consejo Nacional de Investigaciones Científicas y Técnicas (CONICET).

Data availability statement

Research data of this study could be made available upon reasonable request.

Conflict of interest

The authors declare no competing financial interest.

References

[1] Pigni NB, Aranibar C, Mas AL, Aguirre A, Borneo R, Wunderlin D, et al. Chemical profile and bioaccessibility of polyphenols from wheat pasta supplemented with partially-deoiled chia flour. *LWT-Food Science and Technology*. 2020; 124: 109134. Available from: doi:10.1016/j.lwt.2020.109134.

[2] León-López L, Reyes-Moreno C, Ley-Osuna AH, Perales-Sánchez JXK, Milán-Carrillo J, Cuevas-Rodríguez EO, et al. Improvement of nutritional and nutraceutical value of nixtamalized maize tortillas by addition of extruded chia flour. *Biotecnia*. 2019; 21(3): 56-66. Available from: doi:10.18633/biotecnia.v21i3.1012.

[3] Lucini Mas A, Brigante FI, Salvucci E, Pigni NB, Martinez LM, Ribotta P, et al. Defatted chia flour as functional ingredient in sweet cookies. How do Processing, simulated gastrointestinal digestion and colonic fermentation affect its antioxidant properties? *Food Chemistry*. 2020; 316: 1-9. Available from: doi:10.1016/j.foodchem.2020.126279.

[4] Coronel EB, Guiotto EN, Aspiroz MC, Tomás MC, Nolasco SM, Capitani MI. Development of gluten-free premixes with buckwheat and chia flours: Application in a bread product. *LWT-Food Science and Technology*. 2021; 141: 110916. Available from: doi:10.1016/j.lwt.2021.110916.

[5] Guiotto E, Tomás M, Haros C. Development of highly nutritional breads with byproducts of chia (*Salvia hispanica* L.) seeds. *Foods*. 2020; 9(6): 819. Available from: doi:10.3390/foods9060819.

[6] Hussein A. Spirulina-enriched pasta as functional food rich in protein and antioxidant. *Biointerface Research Applied Chemistry*. 2021; 11(6): 14736-14750. Available from: doi:10.33263/BRIAC116.1473614750.

[7] Bustos MC, Paesani C, Quiroga F, León AE. Technological and sensorial quality of berry-enriched pasta. *Cereal Chemistry*. 2019: 96(5): 967-976. Available from: doi:10.1002/cche.10201.

[8] Aranibar C, Pigni NB, Martinez M, Aguirre A, Ribotta P, Wunderlin D, et al. Utilization of a partially-deoiled chia flour to improve the nutritional and antioxidant properties of wheat pasta. *LWT-Food Science and Technology*. 2018; 89: 381-387. Available from: doi:10.1016/j.lwt.2017.11.003.

[9] Aranibar C, Aguirre A, Borneo R. Utilization of a by-product of chia oil extraction as a potential source for value addition in wheat muffins. *Journal of Food Science and Technology*. 2019; 56: 4189-4197. Available from: doi:10.1007/s13197-019-03889-1.

[10] Cota-Gastélum AG, Salazar-García MG, Espinoza-López A, Perez-Perez LM, Cinco-Moroyoqui FJ, Martínez-Cruz O, et al. Characterization of pasta with the addition of *Cicer arietinum* and *Salvia hispanica* flours on quality and antioxidant parameters. *Italian Journal of Food Science*. 2019; 31(3): 626-643. Available from: doi:10.14674/IJFS-1355.

[11] Rodrigues Oliveira M, Ercolani Novack M, Pires Santos C, Kubota E, Severo da Rosa C. Evaluation of replacing wheat flour with chia flour (*Salvia hispanica* L.) in pasta. *Ciencias de Alimentos*. 2015; 36(4): 2545-2554. Available from: doi:10.5433/1679-0359.2015v36n4p2545.

[12] Gull A, Prasad K, Kumar P. Drying kinetics of millet, pomace and wheat based pasta and its effect on microstructure, color, water absorption and pasting properties. *Journal of Food Measurent and Characterization*. 2017; 11: 675-684. Available from: doi:10.1007/s11694-016-9437-6.

[13] Brescini A, Ambrogina PM, Marti A. Pasta-making process: A narrative review on the relation between process variables and pasta quality. *Foods*. 2022; 11(3): 256. Available from: doi:10.3390/foods11030256.

[14] Aranibar C, Pigni NB, Martínez ML, Aguirre A, Ribotta PD, Wunderlin DA, et al. Influence of the extraction conditions on chia oil quality and partially defatted flour antioxidant properties. *Journal of Food Science and Technology*. 2022; 59: 1982-1993. Available from: doi:10.1007/s13197-021-05213-2.

[15] AACC. *Methods 16-50, 14-22, 44-19. Approved Methods of the American Association of Cereal Chemists*. 10th ed. St. Paul, Minnesota: American Association of Cereal Chemists; 2000.

[16] Crank J. *The Mathematicsof Diffusion*. Oxford, UK: Clarendon Press; 1975. p.69-88.

[17] Darvishi H, Asl AR, Asghari A, Azadbakht M, Najafi G, Khodaei J, et al. Study of the drying kinetics of pepper. *Journal of the Saudi Society Agricultoral Science*. 2014; 13(2): 130-138. Available from: doi:10.1016/j.jssas.2013.03.002.

[18] Di Rienzo J, Guzmán A, Casanoves F. A multiple-comparisons method based on the distribution of the root node distance of a binary tree. *Journal of Agricultural and Biolorical Environmental Statistics*. 2002; 7: 129-142. Available from: doi:10.1198/10857110260141193.

[19] Shi Q, Zheng Y, Zhao Y. Mathematical modeling on thin-layer heat pump drying of yacon (*Smallanthus sonchifolius*) slices. *Energy Conversion and Management*. 2013; 71: 208-216. Available from: doi:10.1016/j.enconman.2013.03.032.

[20] López-Mejía N, Andrade-Mahecha MM, Martínez-Correa HA. Mathematical modeling of spaghetti drying kinetics enriched with dehydrated squash pulp (*Cucurbita moschata*). *Revista UDCA Actual Divulgación Científica*. 2019; 22(1): 1151. Available from: doi:10.31910/rudca.v22.n1.2019.1151.

[21] Vimercati WC, Araújo C, Macedo LL, Filho AMM, Saraiva SH, Teixeira LJQ, et al. Influence of drying temperature on drying kinetics, energy consumption, bioactive compounds and cooking quality of pasta enriched with spinach. *Journal of Food Process Engineering*. 2020; 43(12): 1-12. Available from: doi:10.1111/jfpe.13571.

[22] Ogawa T, Adachi S. Drying and rehydration of pasta. *Dry Technology*. 2017; 35(16): 1919-1949. Available from: doi:10.1080/07373937.2017.1307220.

[23] Xing X, Hsieh YSY, Yap K, Ang ME, Lahnstein J, Tucker MR, et al. Isolation and structural elucidation by 2D NMR of planteose, a major oligosaccharide in the mucilage of chia (*Salvia hispanica* L.) seeds. *Carbohydrate Polymers*. 2017; 175: 231-240. Available from: doi:10.1016/j.carbpol.2017.07.059.

[24] Liu P, Yu L, Liu H, Chen L, Li L. Glass transition temperature of starch studied by a high-speed DSC. *Carbohydrate Polymers*. 2009; 77(2): 250-253. Available from: doi:10.1016/j.carbpol.2008.12.027.

[25] Moraga G, Martínez-Navarrete N, Chiralt A. Water sorption isotherms and glass transition in strawberries: influence of pretreatment. *Journal of Food Engineering*. 2004; 62(4): 315-321. Available from: doi:10.1016/S0260-8774(03)00245-0.

[26] Coşkun S, Doymaz İ, Tunçkal C, Erdoğan S. Investigation of drying kinetics of tomato slices dried by using a closed loop heat pump dryer. *Heat Mass Transfer*. 2017; 53: 1863-1871. Available from: doi:10.1007/s00231-016-1946-7.

[27] Ismail MH, Khan KA, Ngadisih N, Irie M, Ong SP, Hii CL, et al. Two-step falling rate in the drying kinetics of rice noodle subjected to pre-treatment and temperature. *Journal of Food Processing Preservation*. 2020; 44(11): 1-11. Available from: doi:10.1111/jfpp.14849.

[28] Hellwig M, Kühn L, Henle T. Individual maillard reaction products as indicators of heat treatment of pasta-A survey of commercial products. *Journal of Food Composition and Analysis*. 2018; 72: 83-92. Available from: doi:10.1016/j.jfca.2018.06.009.

[29] Zhang Y-Q, Hui Y, Wang Y, Zhang B, Guo B-L, Zhang G-Q, et al. Effects of drying temperature and relative humidity on quality properties of chinese dried noodles. *Journal of Food Quality*. 2020; 2020: 1-9. Available from: doi:10.1155/2020/8843974.

[30] Zhou M, Xiong Z, Cai J, Xiong H. Convective air drying characteristics and qualities of non-fried instant noodles. *International Journal of Food Engineering*. 2015; 11(6): 851-860. Available from: doi:10.1515/ijfe-2015-0108.

[31] Mercier S, Villeneuve S, Mondor M, Des Marchais LP. Evolution of porosity, shrinkage and density of pasta fortified with pea protein concentrate during drying. *LWT-Food Science and Technology*. 2011; 44(4): 883-890. Available from: doi:10.1016/j.lwt.2010.11.032.